



LAWRENCE
LIVERMORE
NATIONAL
LABORATORY

Local Magnitude Tomography in California

S. R. Ford, R. A. Uhrhammer, M. Hellweg

May 26, 2010

Bulletin of the Seismological Society of America

Disclaimer

This document was prepared as an account of work sponsored by an agency of the United States government. Neither the United States government nor Lawrence Livermore National Security, LLC, nor any of their employees makes any warranty, expressed or implied, or assumes any legal liability or responsibility for the accuracy, completeness, or usefulness of any information, apparatus, product, or process disclosed, or represents that its use would not infringe privately owned rights. Reference herein to any specific commercial product, process, or service by trade name, trademark, manufacturer, or otherwise does not necessarily constitute or imply its endorsement, recommendation, or favoring by the United States government or Lawrence Livermore National Security, LLC. The views and opinions of authors expressed herein do not necessarily state or reflect those of the United States government or Lawrence Livermore National Security, LLC, and shall not be used for advertising or product endorsement purposes.

Local Magnitude Tomography in California

Sean R. Ford, Robert A. Uhrhammer, and Margaret Hellweg

Abstract

Lateral variation in crustal attenuation of California is calculated by inverting 25,330 synthetic Wood-Anderson amplitudes from the California Integrated Seismic Network (CISN) for site, source, and path effects. Two-dimensional attenuation (q or $1/Q$) is derived from the path term, which is calculated via an iterative least-squares inversion that also solves for perturbations to the site and source terms. Source terms agree well with initial CISN M_L s and site terms agree well with a prior regression analysis. q ranges from low attenuation at 0.001 ($Q = 1000$) to high attenuation at 0.015 ($Q = 66$) with an average of 0.07 ($Q = 143$). The average q is consistent with an amplitude decay function ($\log A_0$) for California when q is combined with a simple geometrical spreading rate. Attenuation in California is consistent with the tectonic structure of California, with low attenuation in the Sierra batholith and high attenuation at The Geysers, at Long Valley, and in the Salton Trough possibly due to geothermal effects. Also, path terms are an order of magnitude smaller than site and source terms, suggesting that they are not as important in correcting for M_L .

Online material: Test of isotropic radiation assumption and L-curve analysis.

Introduction

An understanding of regional attenuation can help when interpreting of tectonic features, especially their thermal structure and water content. These features have a greater influence on attenuation than velocity, which is more commonly measured. The calculation of laterally varying (two-dimensional, 2D) attenuation can also help to constrain earthquake parameters that depend on amplitude like event magnitude. Previous studies of attenuation in California have been made for one-dimensional (e.g., Erickson et al. (2004); Ford et al. (2008)) and 2D (e.g., Mayeda et al. (2005); Phillips and Stead (2008)) cases.

In this study we make use of recent work to recalibrate the CISM local magnitude (M_L) scale (Hellweg et al., 2007). The project required the calculation of Wood-Anderson amplitudes measured at stations of the CISM for a good distribution of earthquakes, which resulted in over 30,000 amplitude measurements. Inspired by the work of Pei et al. (2006), we perform an M_L tomographic study of California and invert the amplitudes for source, site and path effects. M_L tomography provides a unique data set and perspective for examining the crust and attenuation in the frequency band that affects ordinary structures. We discuss the resultant terms and assess their significance in relation to California tectonics and the measurement of M_L .

Data and Method

The M_L recalibration study for the CISM (Hellweg et al. (2007)) used events with catalog $M_L \geq 3.0$ that occurred between 2000 and 2006, and in order to get an even distribution, the largest event in a 50 km grid was selected. In an attempt to obtain more recent measurements, a

second pass along this grid was made for events that occurred in 2006. This resulted in more than 200 events. Data at distances between 1 and 500 km from these events measured on the horizontal components was obtained from over 300 strong-motion and broadband stations of the northern and southern California networks, as well as some data from temporary deployments of the USArray. The Wood-Anderson seismograph response of these data were calculated (Uhrhammer et al. 1996) and the maximum amplitude on the trace was measured.

For this study, in order to obtain a more even magnitude distribution, data for events with $M > 5.5$ were discarded. All events were recorded at more than one station. Also, if a station recorded an event with more than one instrument (strong-motion and broadband) the components were averaged so that each station had exactly two horizontal measurements. These criteria resulted in 185 events recorded at 335 stations (670 components) for 25330 amplitude measurements, which produced a very dense sampling of California (Figure 1a).

We employ the tomography method of Phillips and Stead (2008) where the Wood-Anderson amplitude A_{WA} at a given distance r and frequency f can be estimated by

$$A_{WA}(f, r) = S(f)R(\theta)P(f)G(r)\exp\left(\frac{-r\pi f}{QU}\right), \quad (1)$$

where $S(f)$ is the source spectrum and $R(\theta)$ is the source radiation in the source-receiver direction θ . $P(f)$ is the site term, and $G(r)$ is the geometrical spreading term. The final term is an apparent attenuation (parameterized by Q), where U is the group velocity of the phase that produces the amplitude measurement. In California, at short distances ($\sim < 80$ km) this phase is the direct

arrival and at greater distance ($\sim > 120$ km) it is a mix of crustal and Moho/surface reflections resulting in Lg . Between these distances (80-120 km) Sn and SmS are strong parts of the amplitude measurement. Despite the changing contributions to the measured amplitude, we make the simplifying assumption of constant U equal to 3.5 km/s. This group velocity is most appropriate for the phases recorded at greater distances, so some error will propagate into measured Q , though this is assumed to be small.

The log transform of eq (1) is

$$\log[A_{WA}(f, r)] = \log[S(f)] + \log[R(\theta)] + \log[P(f)] + \log[G(r)] - \frac{r\pi f}{QU} \quad (2)$$

We adopt a geometrical spreading term from Street et al. (1975) of the following form

$$G(r) = \begin{cases} \frac{1}{r} & r < r_0 \\ \frac{1}{r_0} \left(\frac{r_0}{r} \right)^{0.5} & r \geq r_0 \end{cases} \quad (3)$$

The distance r_0 as well as a starting 1D Q model for California were found by fitting the amplitude decay function ($\log A_0$) used in southern California for determining local magnitude (Kanamori et al., 1999),

$$\log A_0(r) = 1.11 \cdot \log(r) + (0.00189r) + 0.591, \quad (4)$$

which is very similar to the CISN $\log A_0$ calculated by Hellweg et al. (2007), which will be used for all of California. The best fit was given by $r_0=200$ and $Q=150$ (Figure 2), so that the spreading for the maximum amplitude transitions from body-wave (r^{-1}) to surface-wave (\sqrt{r}) at approximately 200 km. We validate the assumption of an approximately isotropic radiation pattern (Figure S1 in the electronic supplement to this article) so that $R(\theta)$ can be approximated by a constant and the amplitudes can be corrected using eq (3) and an initial Q model, then eq (2) can take the form

$$\log[A_{WA}(f_{WA})] = \log[S(f_{WA})] + \log[P(f_{WA})] - \frac{\pi f_{WA}}{U} \int_s Q^{-1} ds \quad (5)$$

where f_{WA} is the frequency band of the synthetic Wood-Anderson amplitudes, which can be approximated as a two-pole highpass Butterworth filter with a corner at 1.25 Hz (Uhrhammer and Collins, 1990), and is assumed to be approximately 1 Hz in this analysis. The form is put into a damped first-difference least-squares inversion (LSQR, Paige & Saunders, 1982) to calculate the source, site, and path terms in the Wood-Anderson band along the incremental ray length, s . We chose a damping coefficient of 150 and a grid-spacing of 0.2° based on an L-curve analysis, where these 2 choices minimized the model length and residual variance satisfactorily (Figure S2 in the electronic supplement to this article).

Results and Discussion

The event terms agree well with catalog magnitudes (Figure 3). The difference between the event terms and catalog magnitudes (event bias) are centered on zero with a standard deviation of 0.25.

Site terms agree very well with station corrections, or station-network-component-location (SNCL) dM_L s (Figure 4). These SNCL dM_L s are obtained from a separate L-1 norm inversion (Hellweg et al., 2007), which required historical corrections to be maintained in the current algorithm. The constraint is evident in the SNCL dM_L histogram, which is shifted off a mean of zero. There are several outliers in this comparison. Two positive term outliers are the Transportable Array (TA) stations, P05C and R05C on the north and east components, respectively. This may be due to the small number of observations made during this temporary installation (ten and five, respectively). The negative term outliers (gray ellipse, Figure 5) each have more than sixty observations, but they are all located near the Long Valley region (Region B, Figure 1b). If the SNCL dM_L s are correct, then the path term in this region is under-predicted, which would result in a greater q (higher attenuation) in this area.

Resolution of the path term is calculated via direct solution of the normal equations using Cholesky decomposition and the resolution length is estimated by taking the square root of the ratio of grid area to diagonal resolution element (Phillips and Stead, 2008). This length is contoured in Figure 1b and is highest in southern California at 0.5° , where the network of stations is dense, but a resolution of 1° is found for most of California.

Q is derived from the path term and ranges from 66 to a little more than 1000 in California. Its inverse, q , is directly related to attenuation and correlates well with geological and topographical regions (Figure 1b). Attenuation is high in the geothermal regions of The Geysers, Long Valley, and the Salton Trough (A, B, and D, respectively, Figure 1a) and low in the Sierra Nevada batholith (C, Figure 1a). As discussed earlier, we may expect q in the Long Valley region to be

even greater. There is a slight suggestion that high q may be associated with regions where faulting is observed. This is most evident along the Garlock Fault (latitude=35°) and possibly the Hayward Fault system (latitude=37.5°, longitude=-121.8°). One of the most unexpected features of the tomogram is the relatively low q region in the San Francisco Bay Area, and several validation tests prove it to be a robust feature. Though absolute Q in this region ($Q \sim 200$) agrees with Mayeda et al. (2005) and the 1-D model for the Bay Area of Malagnini et al. (2007), it differs from previous work by Ford et al., (2008) ($Q \sim 100$). The reason for the discrepancy may be associated with the tectonics of the region. Ford et al. (2008) were careful only to measure attenuation in the Franciscan block (west of the San Andreas Fault), however this study uses paths that traverse both the Franciscan and Salinian blocks (east of the San Andreas Fault). In fact, Phillips et al. (1988) found a distinct difference in coda Q for the two regions, and though the absolute values are different between this study and their results, the ratios of the regions are similar. Furthermore, there is a suggestion in the results of Phillips and Stead (2008) that attenuation in this region may be lower relative to its surroundings.

The path term could act as a third correction for M_L in addition to the $\log A_0$ and SNCL dM_L corrections that are already applied when calculating M_L in California. However, the path correction is an order of magnitude smaller than the $\log A_0$ and SNCL dM_L s (0.01 versus 0.1, respectively). Though, the effect of extreme Q structure in regions like the Sierra Nevada, The Geysers, and the Salton Trough may be large enough to warrant a path correction for paths affected by those regions.

Random error will not greatly affect the results presented here due to the excellent ray coverage and the damping used in the inversion. However, the assumptions employed here, namely isotropic radiation, and straight-line wave propagation that samples the crust will introduce systematic error into the interpretation. The isotropic radiation assumption may affect the data at short (<100 km) distances where the normalizing effects of scattering and dispersion do not play a large role, whereas the wave propagation assumption may affect the data at long (>300 km) distances where the measured amplitude may belong to a diving wave that has sampled the upper mantle. Finally, it is difficult to comment on intrinsic attenuation of crustal material in California because this method measures a path q that is a combination of both intrinsic and scattering attenuation.

Conclusion

We use of over 25,000 amplitude measurements made to recalibrate M_L in California to derive Q from the path term of an amplitude tomography method, which also solves for perturbations to the site and source terms. Source terms agree well with initial CISCN M_L s and site terms agree well with a prior regression analysis (Hellweg et al., 2007). Q ranges from 66 to 1000 with an average of 143. The average Q is consistent with an amplitude decay function ($\log A_0$) for California when combined with a simple geometrical spreading rate. Attenuation in California is consistent with the tectonic structure of California, with high Q in the Sierra batholith and low Q at The Geysers, Long Valley, and Salton Trough possibly due to geothermal effects. There is also increased attenuation along shear zones with active faulting. Our results in the San Francisco Bay Area agree with the 1-D analysis of Malagnini et al. (2007) and 2-D study of

Mayeda et al. (2005). A more complete Q model may aid in ground motion estimates for California. Finally, path terms are an order of magnitude smaller than site and source terms, suggesting that they are not as important in correcting for M_L .

Data and Resources

Amplitude data for California were obtained from the Northern California Earthquake Data Center (NCEDC) and the Southern California Earthquake Data Center (SCEDC) as part of the forthcoming California Integrated Seismic Network (CISN) earthquake magnitude reconciliation project. Some plots were made using the Generic Mapping Tools version 4.2.2 (www.soest.hawaii.edu/gmt; Wessel and Smith, 1998).

Acknowledgements

This work was performed under the auspices of the Lawrence Scholar Program and the U.S. Department of Energy by Lawrence Livermore National Laboratory under Contract DE-AC52-07NA27344. This is BSL contribution 10-XX.

Figures

Figure 1. a) Inset, data coverage map of California, where grid nodes (0.2°) are shaded according to number of paths crossing them. Events (circles, $N=185$) and stations (crosses, $N=335$) used in

the analysis are also shown. b) Local magnitude tomography of California. The scale is given in Q , and q ($1/Q$), where hot colors (red) are high attenuation and cool colors (blue) are low attenuation. Regions discussed in text are annotated: A) Geysers, B) Long Valley, C) Sierra Nevadas, D) Salton Trough.

Figure 2. Amplitude decay and attenuation functions. Dark solid line is the $\log A_0$ used in southern California (Kanamori, 1999), which is very similar to one derived for all of California (Hellweg et al, 2007). Dashed line is the geometrical spreading function given in eq (3). Light solid line is a constant Q of 150 and dashed light line is the combination of the geometrical term and the constant Q plus $K=0.73$.

Figure 3. Event term compared to catalog magnitude (CISN ML). Histograms along the axes show the distributions of the event terms (top) and catalog magnitudes (right). The event terms from the inversion agree well with the catalog magnitudes.

Figure 4. Station term compared to regression result for station-network-component-location (SNCL) dML. Histograms along the axes show the distributions of the station terms (top) and the SNCL dMLs (right). The station terms agree well with the regression result, but the mean is shifted toward zero (as prescribed by the inversion). Two outliers (gray crosses) with a small number of observations are annotated and another cluster of outliers is shown by the gray ellipse.

Figure S1. Corrected amplitude (crosses) variation with a) azimuth and b) distance for the 5 Feb 05 Alum Rock ($M_w 4.1$) earthquake. The radial (dashed line) and tangential (solid line) radiation

pattern of the event is plotted in a) and the Kanamori et al. (1999) $\log A_0$ is plotted in b) (for which the amplitudes have been corrected). The gray region in b) is the mean magnitude $(4.43) \pm 2\sigma$ ($\sigma=0.36$), where the white line is the calculated M_W . The catalog M_L for this event is 4.42.

Figure S2. L-curve analysis, where the damping coefficient used in the inversion that produced the model and residuals is given for grid spacing of 0.2° . The gray line is for a grid spacing of 0.1° . A damping coefficient of 150 was selected (bold type) because it minimizes the root-mean-square (RMS) of the model and residual.

Berkeley Seismological Laboratory
(S.R.F., R.A.U., M.H.)

References

- Ford, S. R., D. S. Dreger, K. Mayeda, W. R. Walter, L. Malagnini, and W. S. Phillips (2008). Regional attenuation in Northern California: A comparison of five 1D Q methods, *Bull. Seis. Soc. Amer.* **98** (4) 2033-2046, doi: 10.1785/0120070218.
- Erickson, D., D. E. McNamara, and H. M. Benz (2004). Frequency-dependent L_g Q within the continental United States, *Bull. Seis. Soc. Amer.*, **94**, 1630-1643.
- Hellweg, M., R. A. Uhrhammer, K. Hutton, A. Walter, P. Lombard and E. Hauksson (2007). Recalibrating ML for CISN, *Eos Trans. AGU*, **88** (52), Fall Meet. Suppl., Abstract S41B-0565.

244 Kanamori, H., P. Maechling, and E. Hauksson (1999). Continuous monitoring of ground-motion
 245 parameters, *Bull. Seis. Soc. Amer.* **89** (1) 311-316.

246 Malagnini, L., K. Mayeda, R. Uhrhammer, A. Akinci, and R. B. Herrmann (2007). A regional
 247 ground-motion excitation/attenuation model for the San Francisco region, *Bull. Seis. Soc.*
 248 *Amer.* **97** (3) 843-862, doi: 10.1785/0120060101.

249 Mayeda, K., L. Malagnini, W. S. Phillips, W. R. Walter, and D. S. Dreger (2005). 2-D or not 2-
 250 D, that is the question: A northern California test, *Geophys. Res. Lett.* **32** (L12301),
 251 doi:10.1029/2005GL022882.

252 Paige, C. C., and M. A. Saunders (1982). Algorithm 583, LSQR: Sparse linear equations and
 253 least-squares problems, *Trans. Math Software*, **8**, 195-209.

254 Pei, S. J. Zhao, C. A. Rowe, S. Wang, T. M. Hearn, Z. Xu, H. Liu, and Y. Sun (2006). ML
 255 amplitude tomography in North China, *Bull. Seis. Soc. Amer.* **96** (4A) 1560-1566, doi:
 256 10.1785/0120060021.

257 Phillips, W. S., W. H. K. Lee, and J. T. Newberry (1988) Spatial variation of crustal coda Q in
 258 California, *Pure Appl. Geophys.* **128** (1-2), 251-261.

259 Phillips, W. S. and R. J. Stead (2008). Attenuation of Lg in the western US using the USArray,
 260 *Geophys. Res. Lett.* **35** (L07307), doi:10.1029/2007GL032926.

261 Street, R. L., R. B. Herrmann, and O. W. Nuttli (1975). Spectral characteristics of the L_g wave
 262 generated by central United States earthquakes, *Geophys. J. R. Astro.* **41**, 51-63.

- 263 Uhrhammer, R. A., and E. R. Collins (1990). Synthesis of Wood-Anderson seismograms from
264 broadband digital records, *Bull. Seis. Soc. Amer.* 80, 702 - 716.
- 265 Uhrhammer, R. A., S. J. Loper, and B. Romanowicz (1996). Determination of local magnitude
266 using BDSN broadband records, *Bull. Seis. Soc. Amer.* 86 (5), 1314-30.

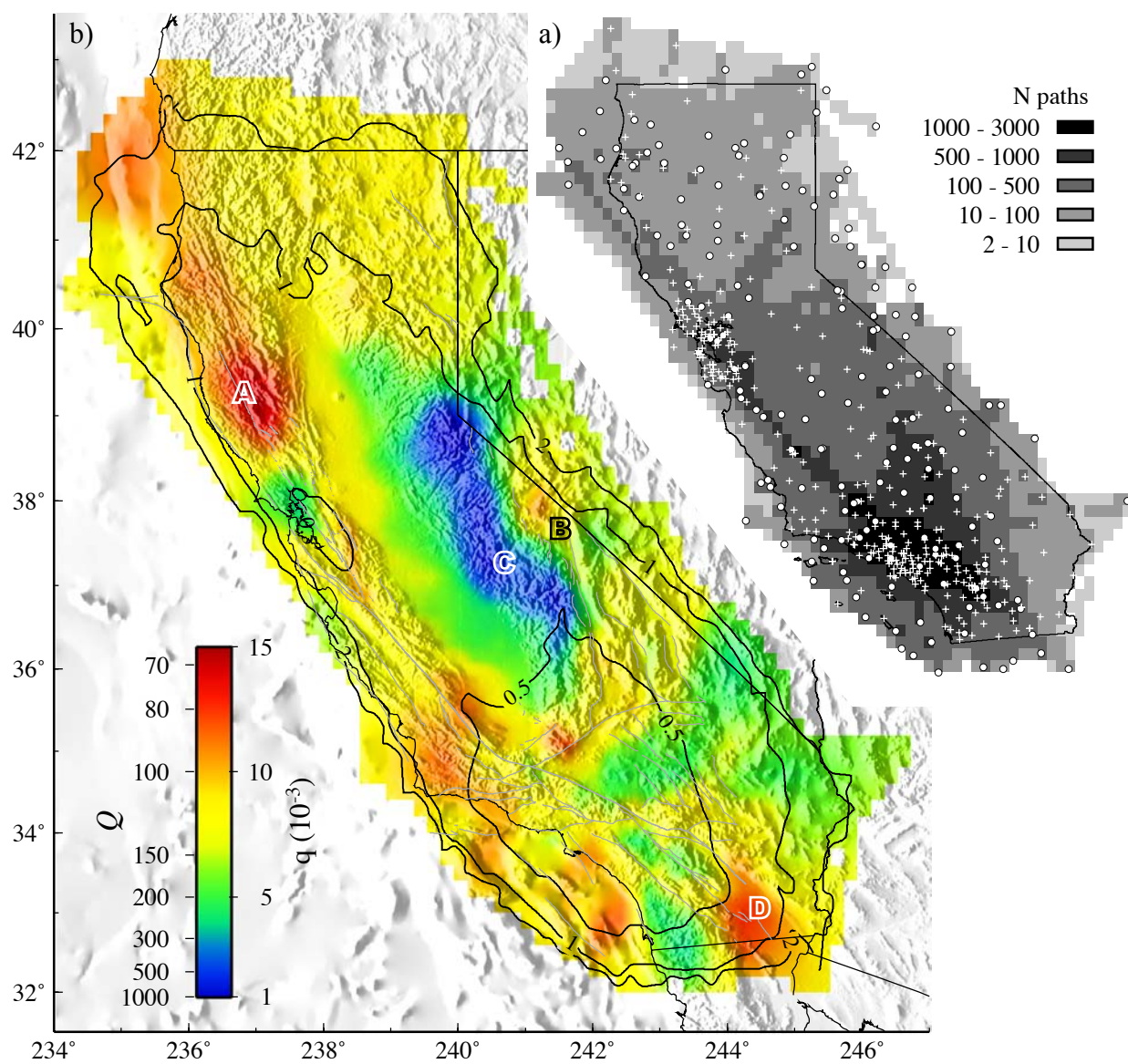


Figure 1.
Ford et al. (2009)
Version 1

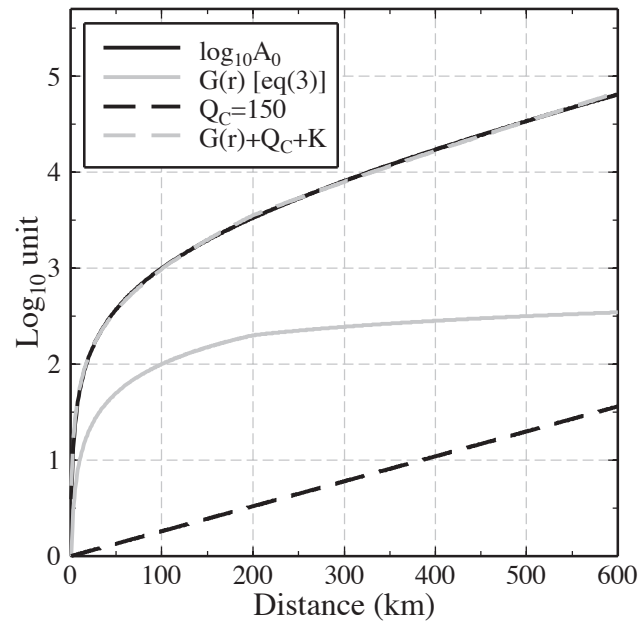


Figure 2.
Ford et al. (2009)
Version 1

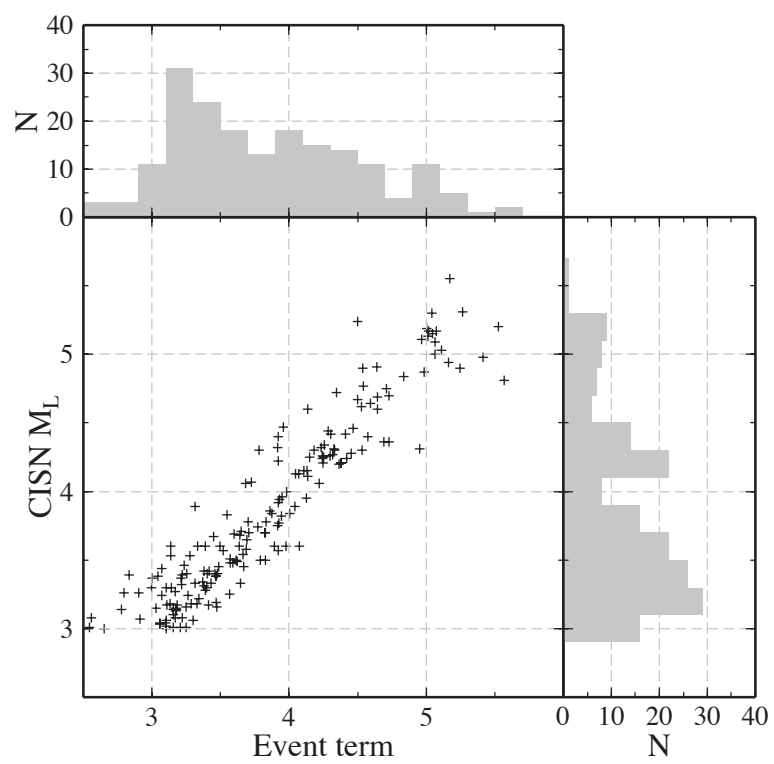


Figure 3.
 Ford et al. (2009)
 Version 1

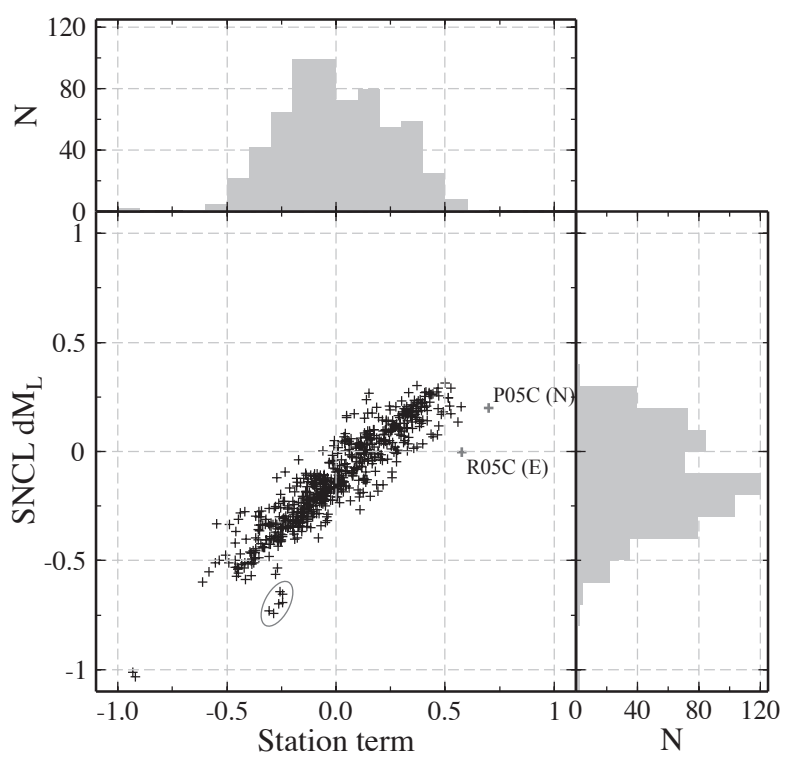


Figure 4.
 Ford et al. (2009)
 Version 1